

Supporting Information

Coordinative chain transfer copolymerization of ethylene and styrene using an *ansa*-bis(fluorenyl) neodymium complex and a dialkylmagnesium

Winnie Nzahou Ottou,^a Sébastien Norsic,^a Marie-Noëlle Poradowski,^b Lionel Perrin,^{*,b} Franck D'Agosto,^{*,a} Christophe Boisson^{*,a}

Université de Lyon, Univ. Lyon 1, CPE Lyon, CNRS UMR 5265, Laboratoire de Chimie Catalyse Polymères et Procédés (C2P2), Equipe LCPP Bat 308F, 43 Bd du 11 Novembre 1918, F-69616 Villeurbanne, France..

Université de Lyon, Université Claude Bernard Lyon 1, CPE Lyon, INSA Lyon, ICBMS, CNRS UMR 5246, Equipe ITEM, 43 Bd. du 11 Novembre 1918, 69622 Villeurbanne, France

Contents

Materials.....	S2
Characterizations technique	S2
General polymerization procedure.....	S3
Influence of styrene concentration (HT-SEC chromatograms)	S5
Influence of magnesium concentration (¹ H NMR spectra).....	S6
Kinetic investigation of the copolymerization.....	S8
Additional HT-SEC chromatograms and NMR spectra (¹ H and ¹³ C).....	S9
Information associated with computational study.....	S13
Computational details.....	S13
Cartesian coordinates of optimized structures and associated energies.....	S13
Additional figures for computational study.....	S14

Materials. All reactions involving air-sensitive compounds were carried out under a protective atmosphere of argon with dry oxygen-free solvents. Prior to use, reaction flasks were dried in vacuum. Toluene was degassed by argon purging and purified with an SPS800 MBraun solvent purification system. Di-*n*-butyl ether (Bu₂O, Sigma-Aldrich) was distilled over sodium/benzophenone and stored under argon before use. Styrene (Sigma-Aldrich) was distilled over CaH₂ and stored in a fridge at -20 °C. *n*-Butyl-*n*-octylmagnesium (BOMAG, Chemtura as a 0.88M solution in heptane) was used as received. The neodymium complex $\{(\text{Me}_2\text{Si}(\text{C}_{13}\text{H}_8)_2)\text{Nd}(\mu\text{-BH}_4)[(\mu\text{-BH}_4)\text{-Li}(\text{THF})]_2\}$ (Nd^{bisflu}) was synthesized using the procedure described previously.¹ Iodine crystals (Sigma-Aldrich) were stored in a glovebox and used as received.

Tetrachloroethylene (TCE, Sigma-Aldrich) was purified by distillation and dried over 3 Å molecular sieves. Deuterated solvents (Eurisotop) were used as received (except CD₃OD which was degassed and stored under argon atmosphere)

Characterizations techniques

Nuclear magnetic resonance (NMR). High-resolution liquid NMR spectroscopy was carried out with a Bruker DRX 400 spectrometer operating at 400 MHz for the ¹H nucleus, and 101 MHz for ¹³C. Spectra were recorded at 363 K using a 5 mm QNP probe for ¹H NMR, and a PSEX 10 mm probe for ¹³C NMR. Polymer samples were examined as 5-15 % (w/v) solutions. A mixture of tetrachloroethylene (TCE) and deuterated benzene (C₆D₆) (2/1 v/v) was used as solvent. Chemical shift values are given in units of ppm, relative to an internal reference of tetramethylsilane for ¹H NMR and to the methylenes of the PE chain at 30 ppm for the ¹³C NMR.

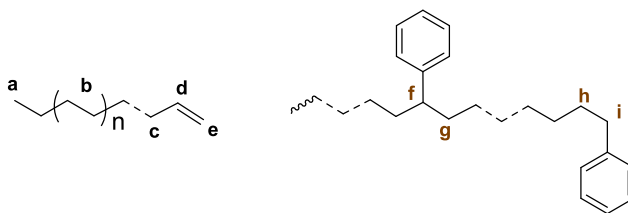
Size Exclusion Chromatography (SEC). High-temperature size exclusion chromatography (HT-SEC) analyses were performed using a Viscotek system (from Malvern Instruments) equipped with three columns (PLgel Olexis 300 mm × 7 mm i.d. from Agilent Technologies). Portions (200 μL) of sample solutions with concentrations of 5 mg mL⁻¹ were eluted in 1,2,4- trichlorobenzene using a flow rate of 1 mL min⁻¹ at 150 °C. The mobile phase was stabilized with 2,6-di-tert-butyl-4-methylphenol (200 mg.L⁻¹). The OmniSEC software was used for data acquisition and data analysis. The molar mass distributions were calculated with a calibration curve on the basis of narrow poly(ethylene) standards (*M_p* : 170, 395, 750, 1110, 2155, 25000, 77500, 126000 g.mol⁻¹) from Polymer Standards Service (Mainz, Germany).

Differential Scanning Calorimetry (DSC). Experiments were performed under argon using a Mettler Toledo DSC 1. All samples were melted at 180 °C for 15 min to erase all thermal history, then cooled to 25 °C, and heated to 180 °C at a rate of 10 °C min⁻¹. The degree of crystallinity X_c was determined considering the melting enthalpy for the 100 % crystalline PE $\Delta H_m = 293 \text{ J g}^{-1}$.

General polymerization procedure. Polymerization was carried out in a 500 mL glass reactor under anoxic, aprotic conditions, with ethylene supplied *via* a 2.13 L ballast chamber to monitor consumption. The required amount of BOMAG (based on the targeted M_n^{theo}) was diluted with toluene (400 mL) followed by addition of 10 equivalent of Bu_2O (relative to Mg) and 5 mL of styrene was then added.

The resulting solution was transferred to the reactor under an argon atmosphere. An antechamber was then charged with a solution of $\{(\text{Me}_2\text{Si}(\text{C}_{13}\text{H}_8)_2)\text{Nd}(\mu\text{-BH}_4)[(\mu\text{-BH}_4)\text{-Li}(\text{THF})]\}_2$, $\text{Nd}^{\text{bisflu}}$, (the Nd complex solubilized in 10 mL of BOMAG solution before injection). The reactor was heated at 75 °C and then charged with an ethylene atmosphere at a pressure of 3 bars. The Nd solution was then added to the reactor and the consumption of ethylene monitored. After the targeted consumption of ethylene, the ethylene atmosphere was replaced with argon and the reaction was quenched with methanol. Then, the reactor contents were precipitated in methanol, and the suspension was filtered. The polyethylene recovered was washed several times with methanol and dried under vacuum at 70 °C.

Determination by ¹H NMR of the percentage of chain-ends (-CH₂-Ph, -CH=CH₂ and -CH₃), the average degree of polymerization (X_n), the number-average molar mass M_n^{NMR} .



We consider:

- For the polyethylene part, the integral of methyl protons and the main methylene protons of PE (I_{CH_3} and I_{CH_2} , respectively) and the integral of the vinyl protons ($I_{\text{CH}=\text{CH}_2}$)
- For the styrene part, the integral of the internal methine (I_{CH}) and the terminal methylene protons ($I_{\text{CH}_2\text{Ph}}$)

Determination of the percentage of chain-ends per chain:

- Methyl chain ends ($\text{CH}_3^{\text{term}}$): $\text{mol \% CH}_3^{\text{term}} = \left(\frac{\frac{I_{\text{CH}_3}}{3}}{\frac{1}{2} \left(\frac{I_{\text{CH}=\text{CH}_2}}{3} + \frac{I_{\text{CH}_3}}{3} + \frac{I_{\text{CH}_2\text{Ph}}}{2} \right)} - 1 \right) \times 100$
- Styryl chain ends (CH_2Ph): $\text{mol \% CH}_2\text{Ph} = \frac{\frac{I_{\text{CH}_2\text{Ph}}}{2}}{\frac{1}{2} \left(\frac{I_{\text{CH}=\text{CH}_2}}{3} + \frac{I_{\text{CH}_3}}{3} + \frac{I_{\text{CH}_2\text{Ph}}}{2} \right)} \times 100$
- Vinyl chain ends (V): $\text{mol \% CH}=\text{CH}_2 = \frac{\frac{I_{\text{CH}=\text{CH}_2}}{3}}{\frac{1}{2} \left(\frac{I_{\text{CH}=\text{CH}_2}}{3} + \frac{I_{\text{CH}_3}}{3} + \frac{I_{\text{CH}_2\text{Ph}}}{2} \right)} \times 100$

Determination of percentage of styrene units per chains:

- Internal styrene units (Sty^{int}): $\text{mol \% Sty}^{\text{int}} = \frac{I_{\text{CHPh}}}{I_{\text{CHPh}} + \frac{I_{\text{CH}_2\text{Ph}}}{2} + \frac{I_{\text{CH}_2-2I_{\text{CHPh}}}}{4}} \times 100$
- Terminal styrene units (Sty^{term}): $\text{mol \% Sty}^{\text{term}} = \frac{\frac{I_{\text{CH}_2\text{Ph}}}{2}}{I_{\text{CHPh}} + \frac{I_{\text{CH}_2\text{Ph}}}{2} + \frac{I_{\text{CH}_2-2I_{\text{CHPh}}}}{4}} \times 100$

The total percentage of styrene units per chain (Sty): $\text{Sty} = \text{Sty}^{\text{int}} + \text{Sty}^{\text{term}}$

Considering the number of ethylene units (E) and the number of styrene units (Sty), the average degree of polymerization (X_n) is determined by the equation: $X_n = \frac{E + \text{Sty}}{\frac{1}{2} [\Sigma (CH_3^{\text{term}} + CH_2\text{Ph} + V)]}$ with $E = \frac{I_{\text{CH}_2-2I_{\text{CHPh}}}}{4}$

The molar mass $M_n^{\text{NMR}} = M_0 * X_n$

With $M_0 = \text{Sty} * M_{\text{Sty}} + (1 - \text{Sty}) * M_{\text{Eth}}$ where M_{Sty} and M_{Eth} are the molar masses of styrene and ethylene, respectively.

Influence of styrene concentration (HT-SEC chromatograms)

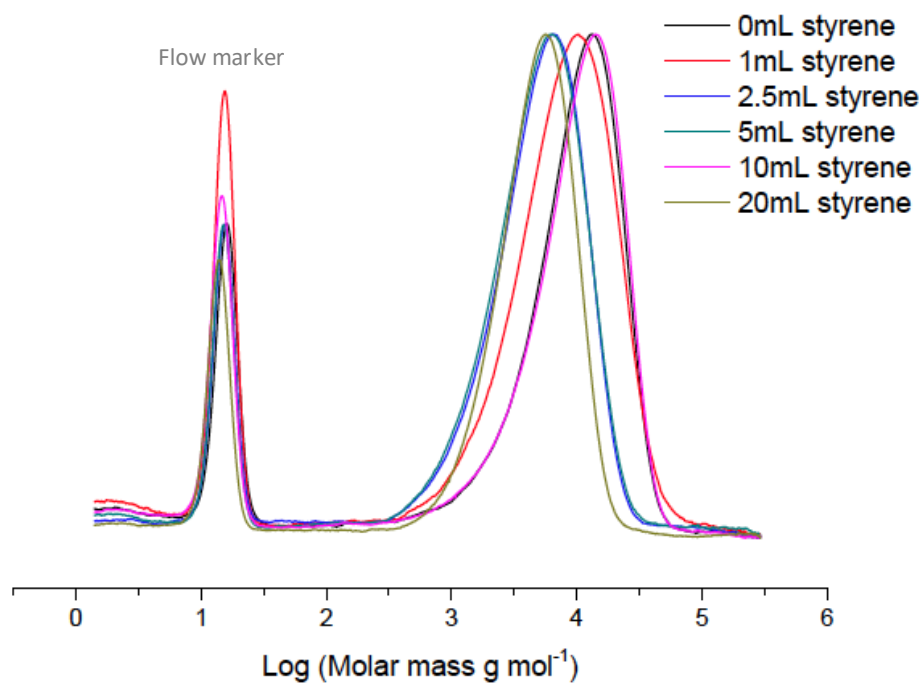


Figure S1. HT-SEC traces (RI) of samples obtained during the copolymerization of ethylene and styrene performed with Nd^{bisFlu}/BOMAG as a catalytic system (Table 1, entries 1-6).

Table S1: Thermal properties of ethylene/styrene copolymers

Entry	Styr ^{int} mol%	Styr ^{term} mol%	M_n^{NMR} (g mol ⁻¹)	Tm ^a (°C)	Xc ^a (%)
1	-	-	5,700	132.9	88
2	0.25	0.02	6,000	128.0	70
3	0.69	0.01	3,700	126.4	60
4	0.78	0.06	2,900	122.7	64
5	2.17	0.03	8,500	121.6	71

[a] Measured by DSC

Influence of magnesium concentration (^1H NMR spectra)

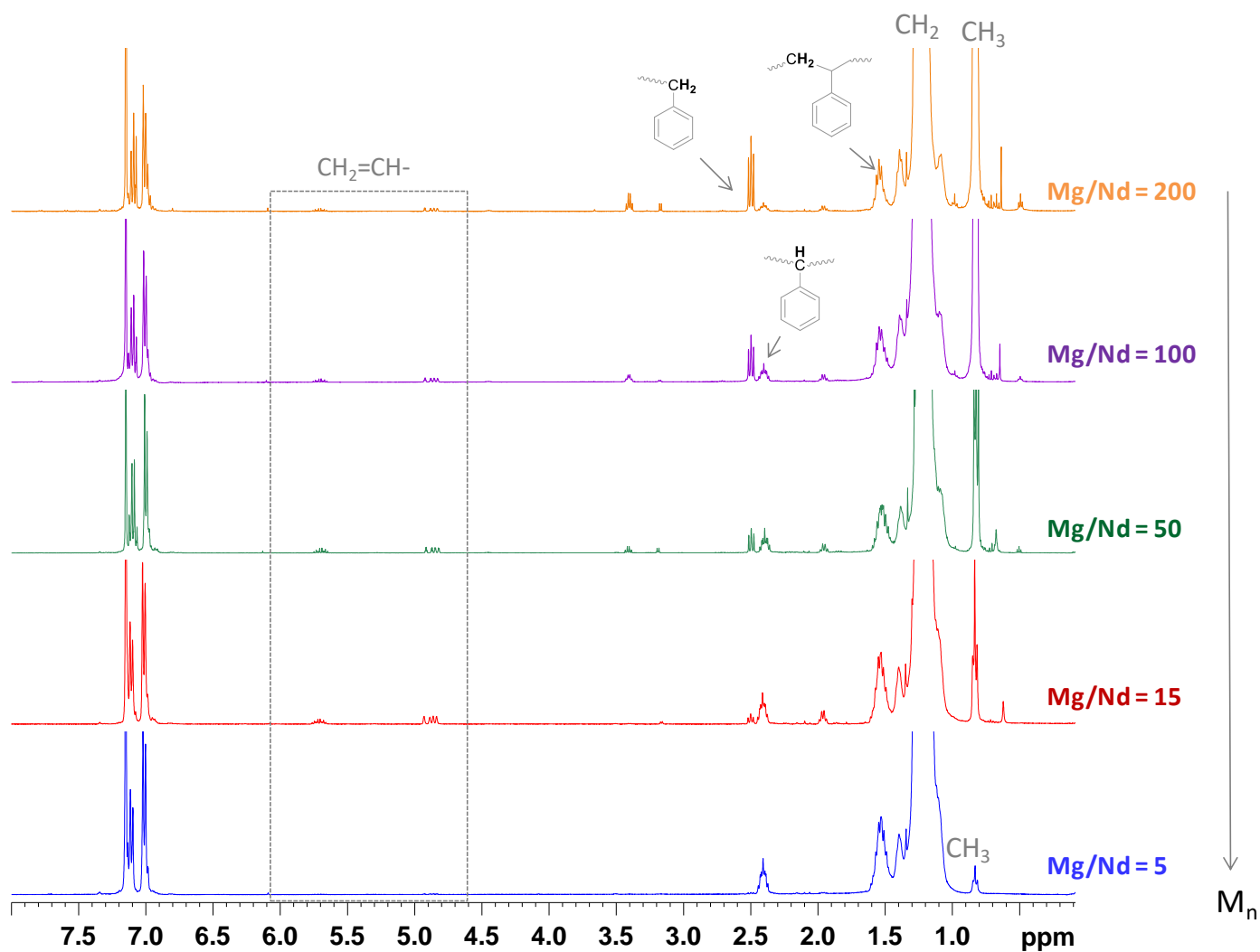


Figure S2. ^1H NMR spectra (TCE/ C_6D_6 , 363 K) of poly(ethylene-co-styrene) obtained with different ratios Mg/Nd (Tables 1-2, entries 11-15 from bottom to top).

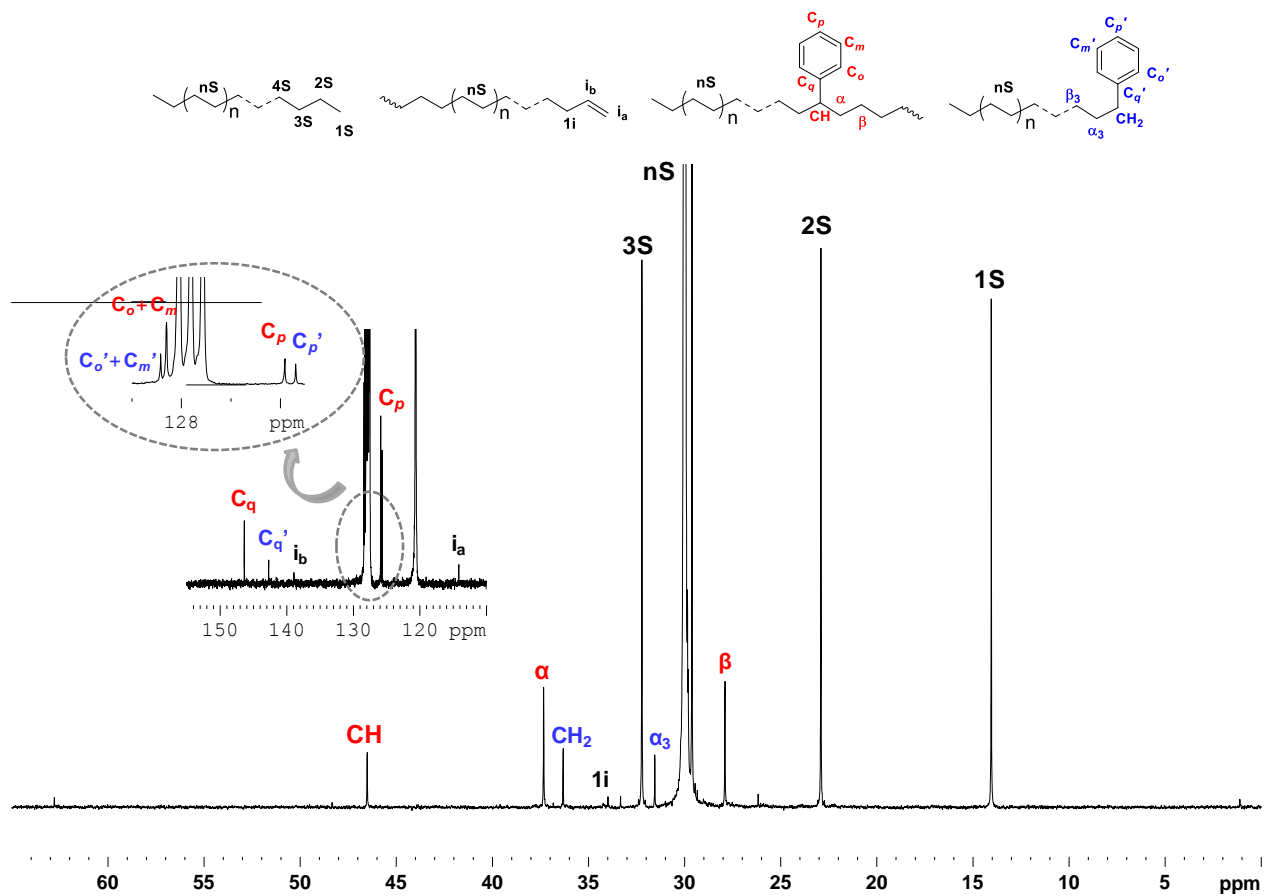


Figure S3. ^{13}C NMR spectrum (TCE/ C_6D_6 , 363 K) of poly(ethylene-co-styrene) obtained with different ratios Mg/Nd (Tables 1-2, entry 14).

Kinetic investigation of the copolymerization

The copolymerization procedure was the same as described above. 8 aliquots were collected at different times and precipitated in MeOH. These samples were then analyzed by ^1H NMR and HT-SEC.

Table S2. Characteristic values of the molar mass distributions and productivities during the copolymerization of ethylene and styrene performed with $\text{Nd}^{\text{bisFlu}}/\text{BOMAG}$ as a catalytic system.

Sample	time (h)	m copolymer (g)	V _{solution} (mL)	Productivity ^a (kg mol ⁻¹)	M _n ^{theo b} (g mol ⁻¹)	M _n ^{NMR c} (g mol ⁻¹)	X _n ^c	M _n ^{SEC d} (g mol ⁻¹)	M _p ^{SEC d} (g mol ⁻¹)	D ^d	nChains/ Mg
1	0.18	0.03	9.18	42.44	210	660	23	560	530	1.4	0.8
2	0.5	0.05	8.86	73.29	370	800	28	700	810	1.4	1.0
3	1	0.06	5.4	144.30	720	1,150	40	1,000	1,270	1.4	1.4
4	2	0.08	4.2	247.37	1,240	1,500	52	1,230	1,740	1.5	2.0
5	4	0.12	3.58	435.32	2,180	3,080	108	1,780	2,540	1.5	2.4
6	6.5	0.25	4.49	723.11	3,620	3,400	118	2,950	4,150	1.4	2.5
7	8	0.23	3.35	891.65	4,460	4,100	143	4,080	5,170	1.4	2.2
8	9	30.98	360.94	1114.69	5,570	5,600	167	4,700	6,900	1.6	2.4

General copolymerization conditions: T = 75°C; 3 bar, V_{toluene} = 400 mL, [Mg]₀ = 7.7 mmol L⁻¹ [Nd]₀ = 77 μmol L⁻¹; [styrene]₀ = 0.11 M (5 mL)

[a] Productivity = $\frac{[\text{COPO}]}{[\text{Nd}]_0}$, where [COPO] is the concentration of poly(ethylene-co-styrene) in the aliquots in kg L⁻¹ and [Nd]₀ the initial concentration of neodymium

[b] Theoretical molar mass $M_n^{\text{theo}} = \frac{[\text{COPO}]}{2 \times [\text{Mg}]_0}$

[c] Determined by ^1H NMR at 363K (TCE/C₆D₆ 2:1)

[d] Determined by SEC in 1,2,4-trichlorobenzene at 150°C using a PE calibration.

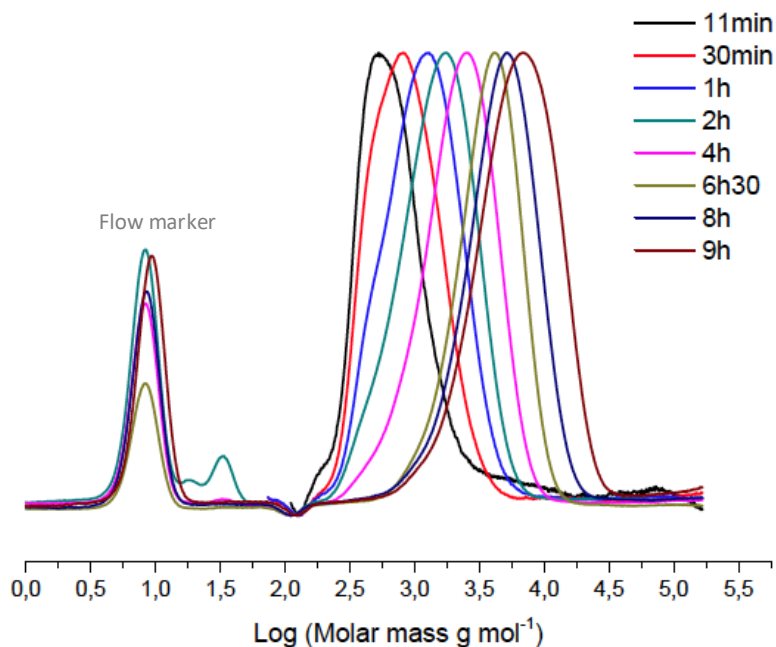


Figure S4. SEC analyses (RI) of samples obtained during copolymerization of ethylene and styrene performed with $\text{Nd}^{\text{bisFlu}}$ /BOMAG as a catalytic system (Table 1, entries 16-23)

Additional HT-SEC chromatograms and NMR spectra (^1H and ^{13}C)

HT-SEC chromatograms and NMR spectra (^1H and ^{13}C) of deuterated poly(ethylene-co-styrene) (*D*-PE)

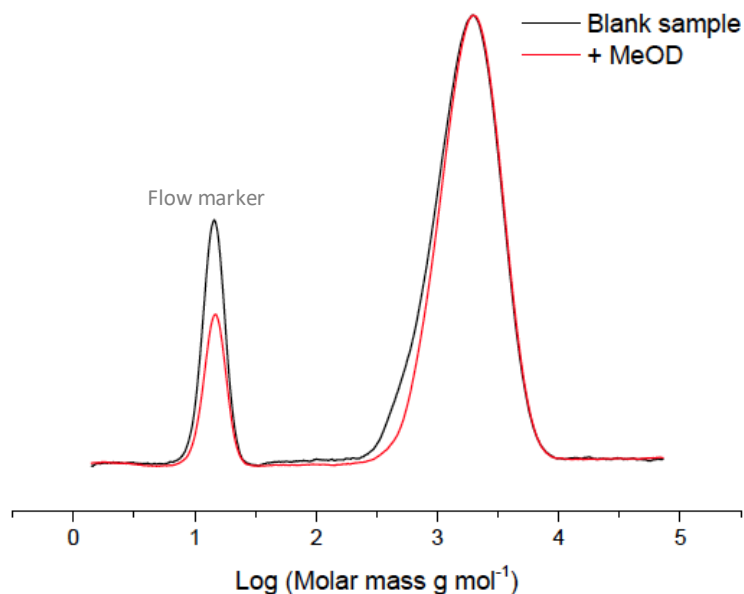


Figure S5. SEC analyses (RI) of poly(ethylene-co-styrene) after addition of CD_3OD to the polymerization medium (Table 3; entries 24-25).

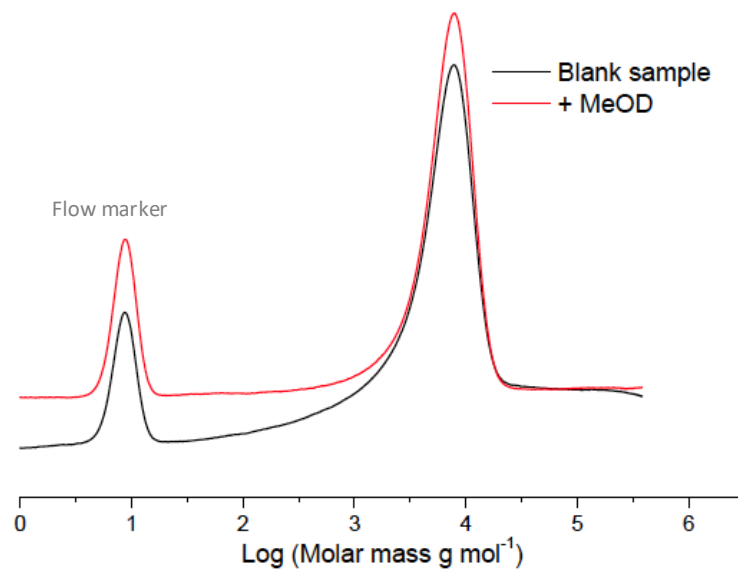


Figure S6. SEC analyses (RI) poly(ethylene-co-styrene) after addition of CD₃OD to the polymerization medium (Table 3; entries 26-27).

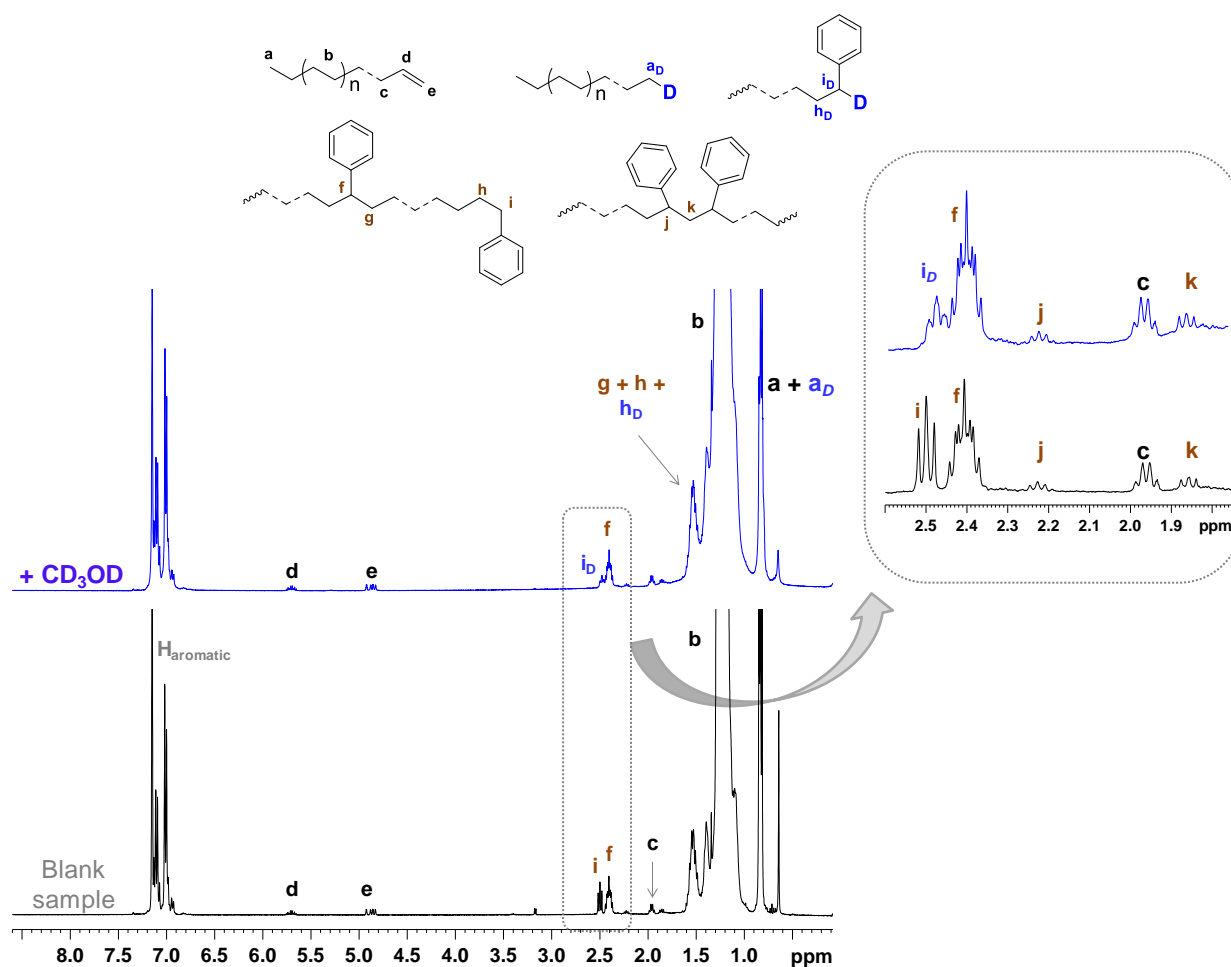


Figure S7. ¹H NMR spectrum (TCE/C₆D₆, 363 K) of poly(ethylene-co-styrene) after addition of CD₃OD to the polymerization medium (Tables 3-4; entries 24-25).

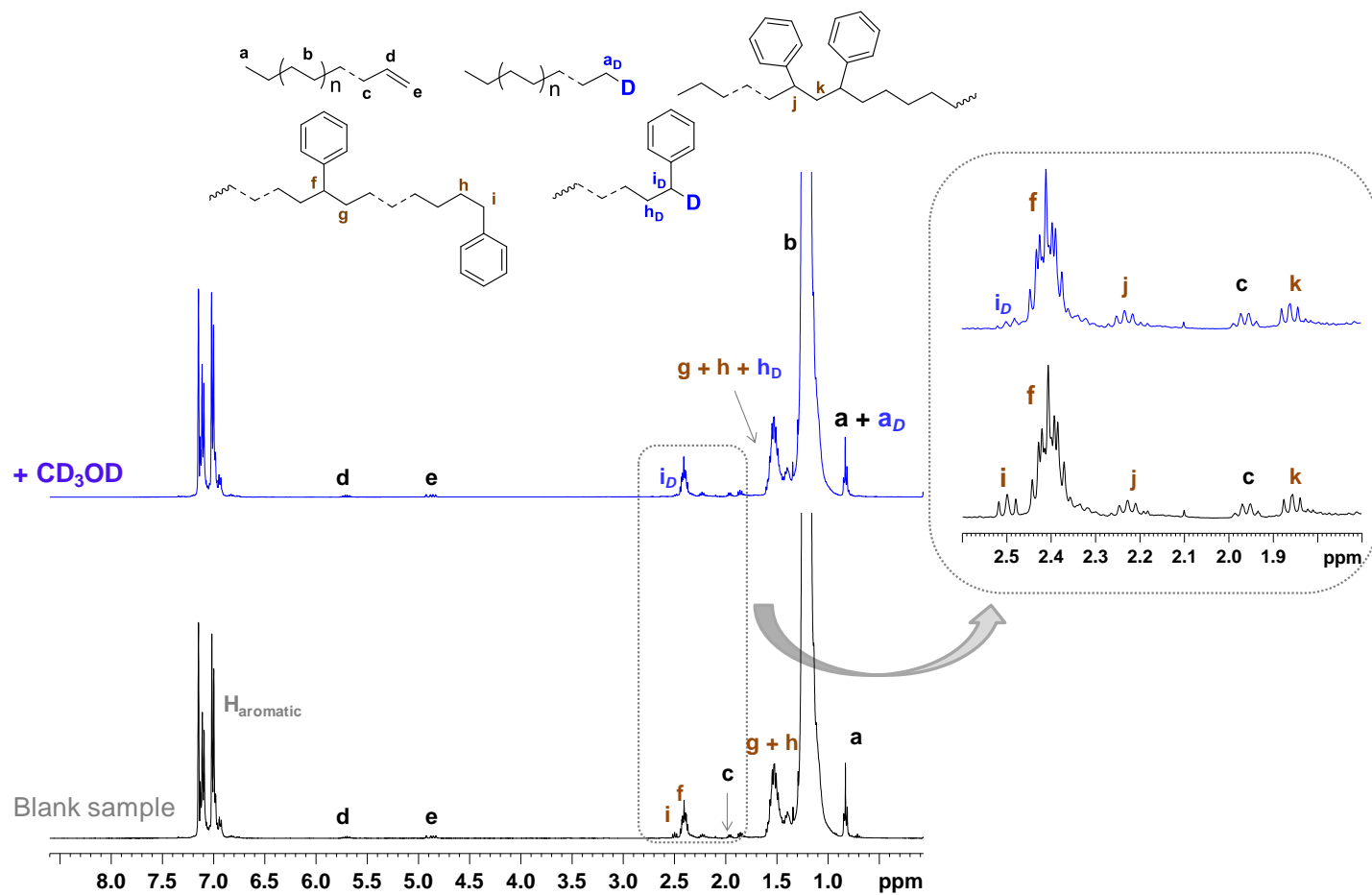


Figure S8. ^1H NMR spectrum (TCE/ C_6D_6 , 363 K) poly(ethylene-co-styrene) after addition of CD_3OD to the polymerization medium (Tables 3-4; entries 26-27).

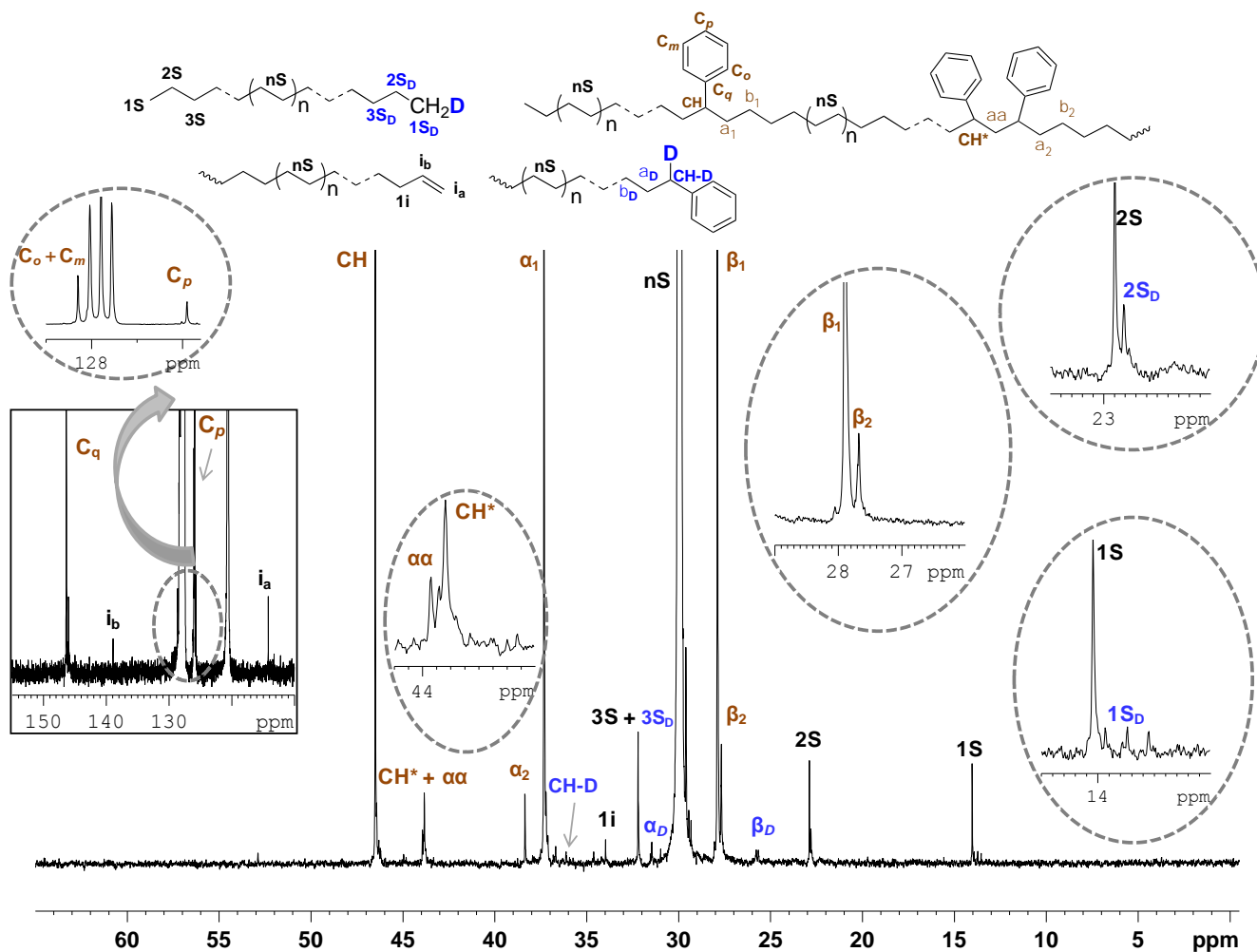


Figure S9. $^{13}\text{C}\{^1\text{H}\}$ NMR spectrum (TCE/ C_6D_6 , 363 K) of poly(ethylene-co-styrene) after addition of CD_3OD to the polymerization medium (Table 3; entry 27).

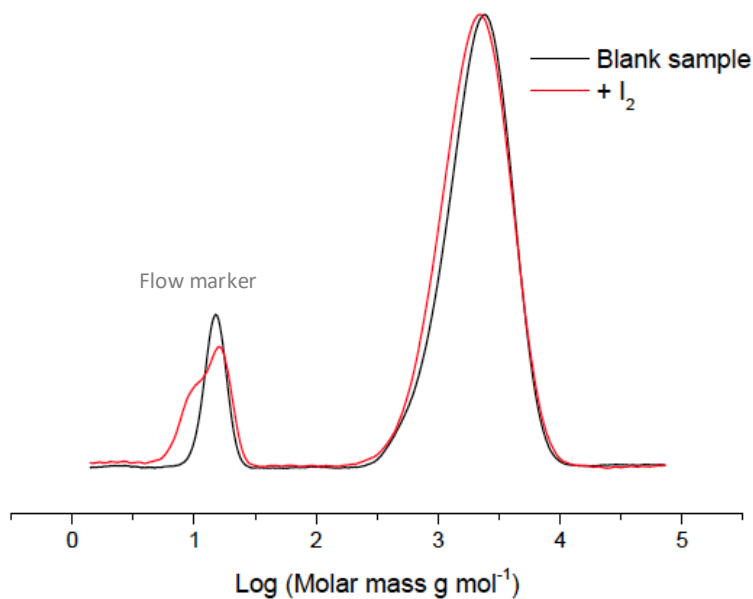


Figure S10. SEC analyses (RI) of poly(ethylene-co-styrene) obtained after addition of I_2 to the polymerization medium (Table 3; entries 28-29)

Supporting information associated with the computational study.

Computational details. Geometry optimization of the minima and transition states were carried out at a DFT level of theory using the hybrid functional B3PW91^{2,3} without any symmetry restrictions. Neodymium was represented by a Stuttgart-Dresden-Bonn quasi-relativistic large effective core potential including the 4f electrons in the core with its associated basis set^{4,5} completed by a polarization f function ($\zeta_f = 1.0$). Silicon was represented by a Stuttgart-Dresden-Bonn pseudopotential and its adapted basis set⁶ augmented by a d function ($\zeta_d = 0.284$). Magnesium was represented by a polarized all electron triple- ζ 6-311G(d,p) basis set and supplemented by a 6 diffuse function.⁷⁻¹⁰ Carbon and hydrogen atoms were represented by a polarized all electron triple- ζ 6-311G(d,p) basis set.⁶⁻⁸ Solvation by toluene was implicitly represented during optimization using the SMD model.¹¹ Single point dispersion correction was taken account using the Grimme empirical correction with the original D3 damping function.¹² Analytical frequency calculations were carried out to verify the nature of the extrema (minimum or transition state). Gibbs energy have been computed within the harmonic approximation and estimated at 298.15 K, 1 atm. Criteria for SCF convergence, geometry optimization and integration grid have been set to default values. All these computations have been performed with the gaussian09 suite of programs (D1 version).¹³

Cartesian coordinates of optimized structures and associated energies. The cartesian coordinates of optimized structures are available in the file ESI.xyz and are readable with Mercury CCDC. The name of each structure and associated energies in a. u. are given on the top of cartesian coordinates. In some cases, the mechanism is dissociative, so the adduct structure is not presented. The structures are named according to the notation presented in the main text and figures. Lowercase letter after S give the conformation (*S* or *R*) of the styrene or styryl unit. The catalyst **Nd**^{bisflu} is labeled SiFlu2.

Additional figures associated with the computational study.

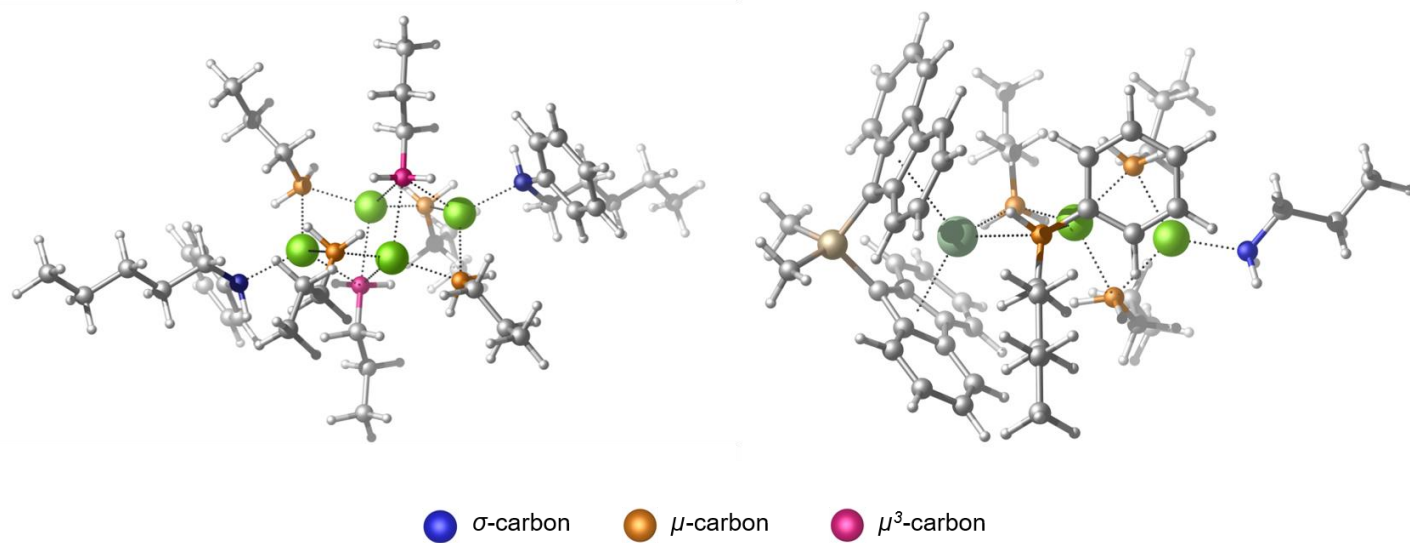
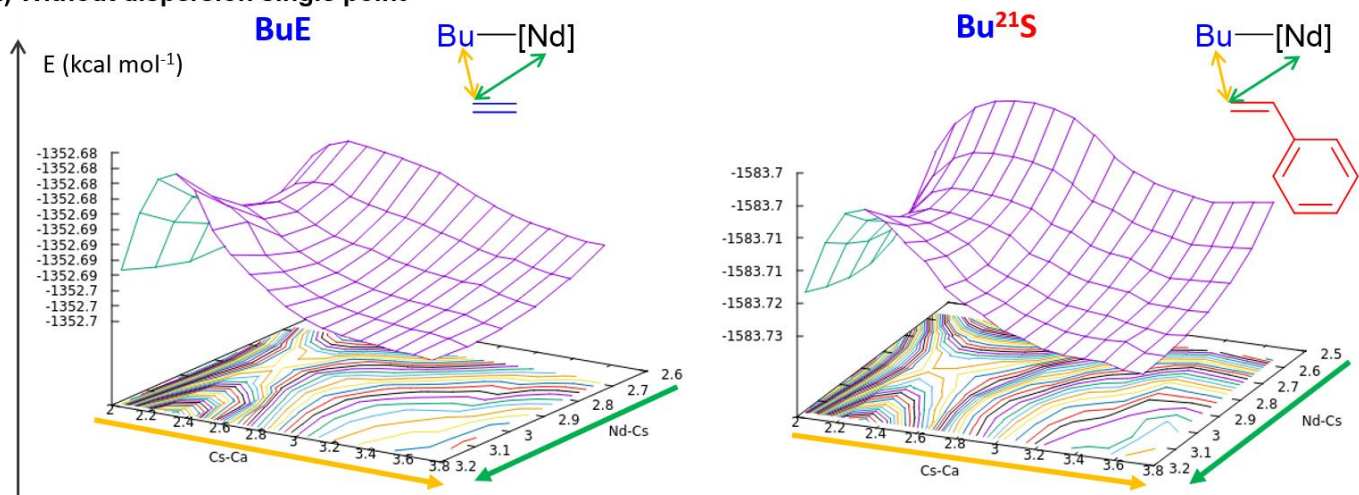


Figure S11. 3D representation of optimized structures of the more stable magnesium cluster without Bu_2O and dormant heterobimetallic species.

a) Without dispersion single point



b) With dispersion single point

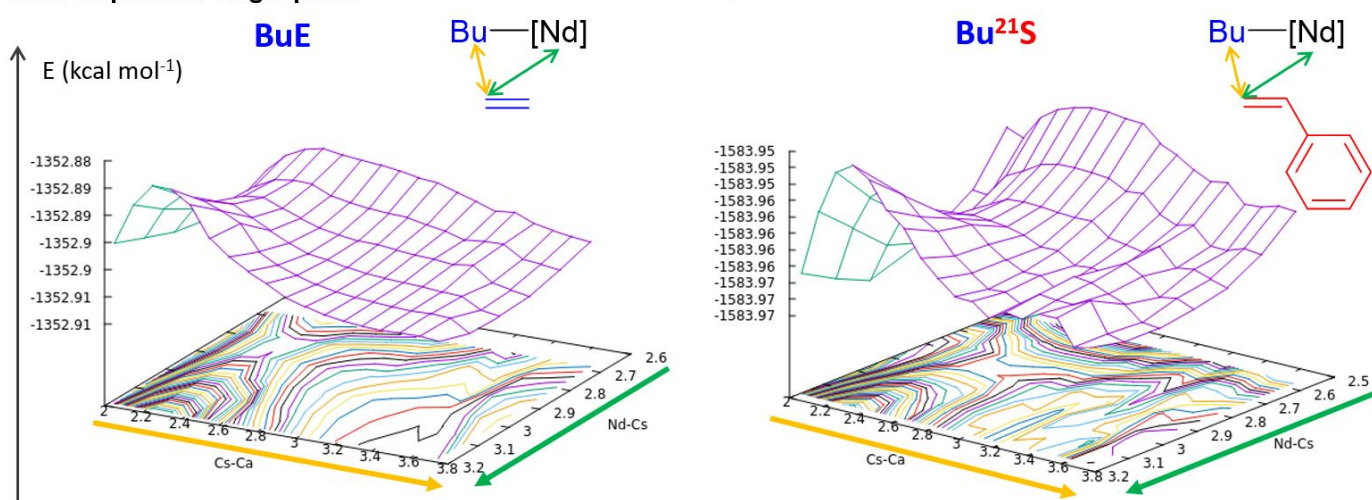


Figure S12. Potential Energy Surface around monomer adducts. The yellow coordinate is the distance of the C-C forming bond and the green coordinate is the distance between the metal center and the monomer carbon. Distance in Angstrom.

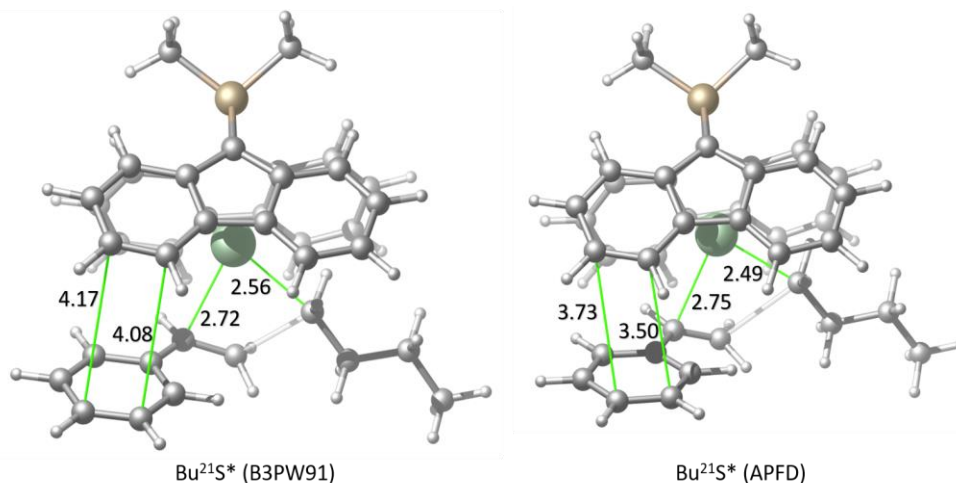


Figure S13. 3D representation of optimized structure of the secondary styrene insertion transition state in the alkyl site. In left, the structure comes from the optimization with the B3PW91 functional and in right, the structure comes from the optimization with the APFD functional. Distances in green in Angstrom.

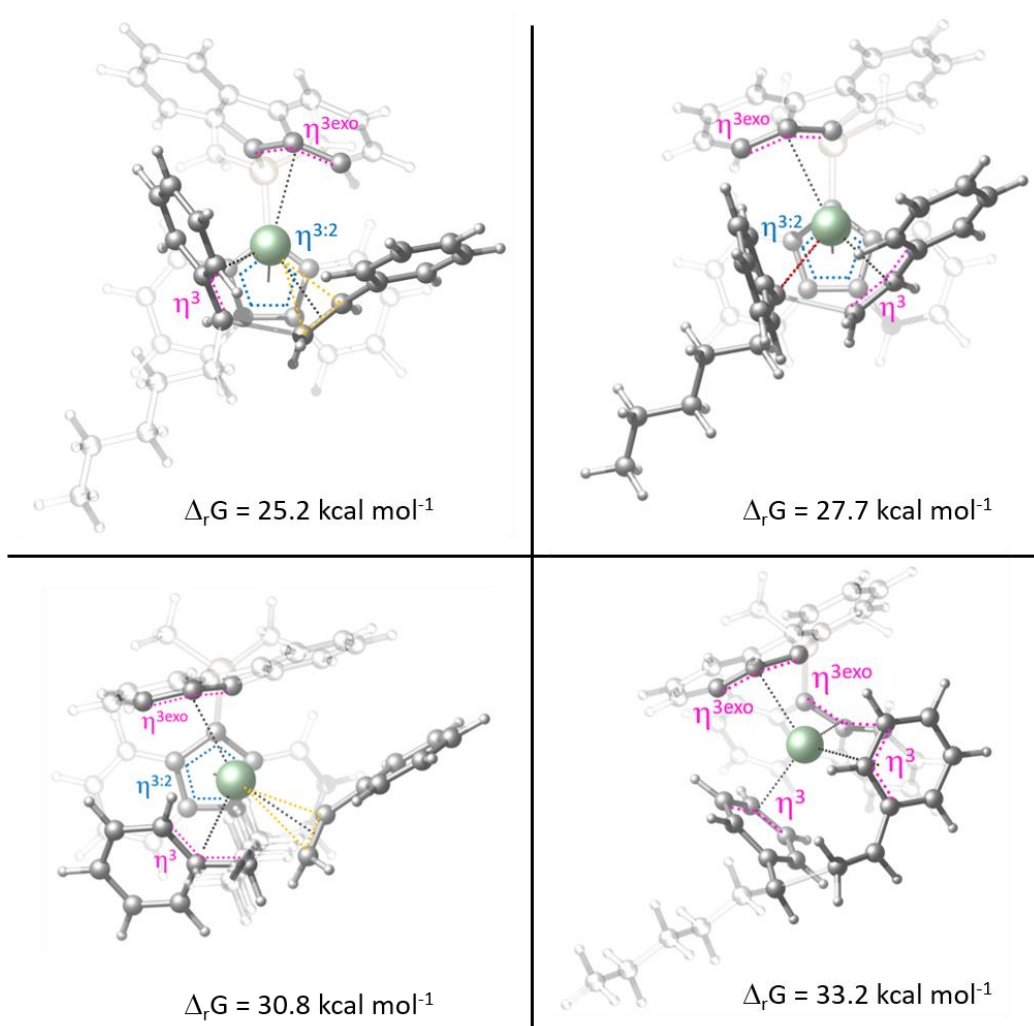


Figure S14. 3D representation of the optimized structure of different transition states in the case of the (*S,R*)- $^{21}\text{S}^{21}\text{S}^*$ insertion. The color dot lines show the hapticity of the metal center. The free energies are given relative to the dormant heterobimetallic species $[\text{Nd}]\text{Mg}_2\text{Bu}_4^{21}\text{S}$.

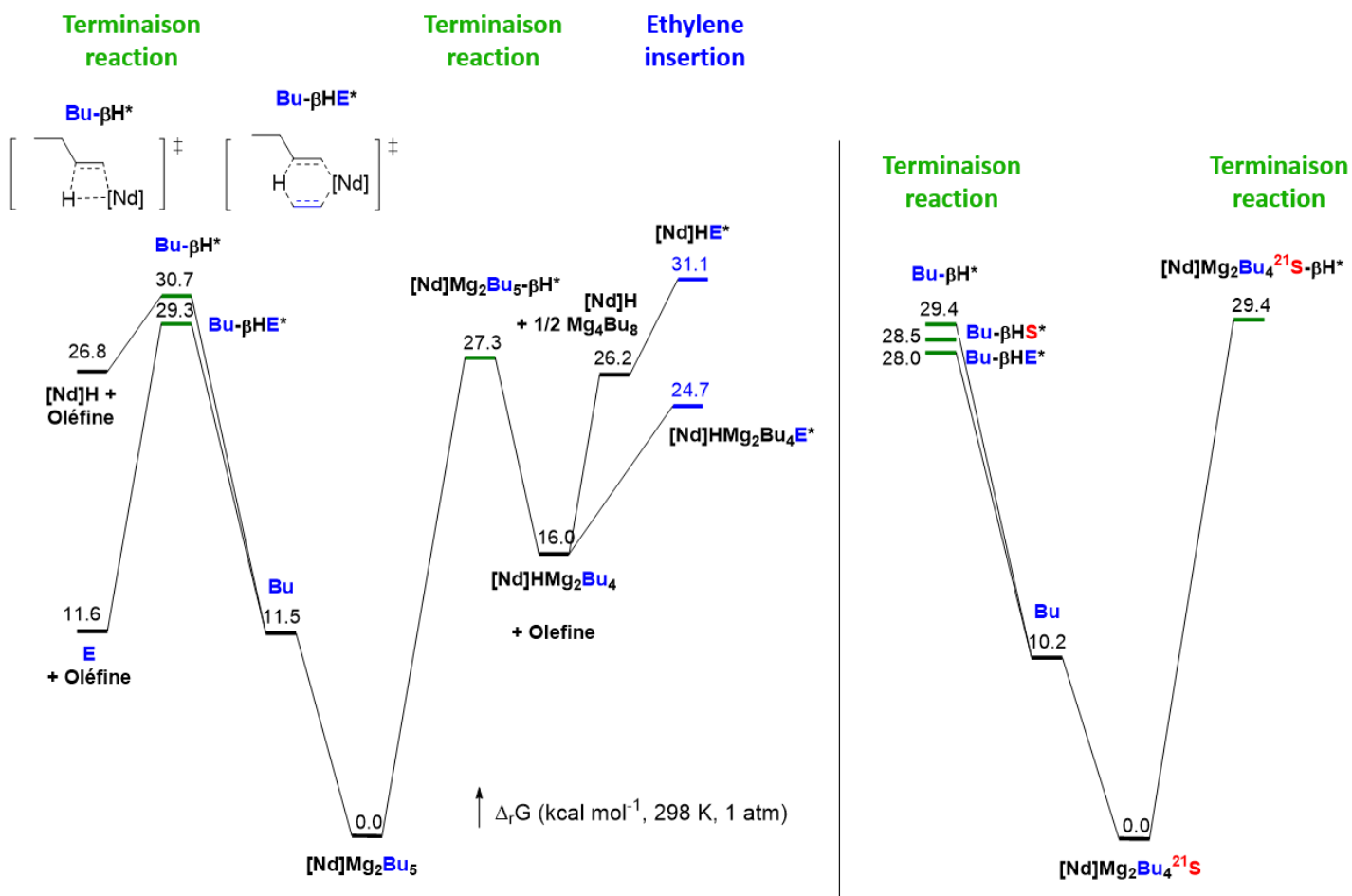


Figure S15. Reactive landscape of termination reactions for the bisalkyl heterobimetallic species $[\text{Nd}]\text{Mg}_2\text{Bu}_5$ (left) and for the alky-styryl heterobimetallic species $[\text{Nd}]\text{Mg}_2\text{Bu}_4^{21}\text{S}$ (right).

References

- 1 J. Thuilliez, L. Ricard, F. Nief, F. Boisson and C. Boisson, *Macromolecules*, 2009, **42** (11), 3774–3779.
- 2 A. D. J. Becke, *Chem. Phys.*, 1993, **98**, 5648–5652.
- 3 J. P. Perdew and Y. Wang, *Phys. Rev. B*, 1992, **45**, 13244–13249.
- 4 M. Dolg, H. Stoll, A. Savin, H. Preuss, *Theor. Chim. Acta*, 1989, **75**, 173–194.
- 5 M. Dolg, H. Stoll and H. Preuss, *Theor. Chim. Acta*, 1993, **85**, 441–450.
- 6 A. Bergner, M. Dolg, W. Kuchle, H. Stoll and H. Preuss, *Mol. Phys.*, 1993, **80**, 1431–1441.
- 7 Krishnan, R.; Binkley, J. S.; Seeger, R.; Pople, J. A. *J. Chem. Phys.* **1980**, **72**, 650–654.
- 8 A. D. McLean and G. S. Chandler, *J. Chem. Phys.*, 1980, **72**, 5639–5648.
- 9 M. J. Frisch, J. A. Pople and J. S. Binkley, *J. Chem. Phys.*, 1984, **80**, 3265–3269.

- 10 T. Clark, J. Chandrasekhar, G. W. Spitznagel and P. V. Schleyer, *J. Comput. Chem.*, 1983, **4**, 294–301.
- 11 A. V. Marenich, C. J. Cramer and D. G. Truhlar, *J. Chem. Theor. Comput.*, 2009, **5**, 2447–2464.
- 12 S. Grimme, J. Antony, S. Ehrlich and H. Krieg, *J. Chem. Phys.*, 2010, **132**, 154104; S. Grimme, S. Ehrlich and L. Goerigk, *J. Comput. Chem.*, 2011, **32**, 1456–1465.
- 13 M. J. Frisch, G. W. Trucks, H. B. Schlegel, G. E. Scuseria, M. A. Robb, J. R. Cheeseman, G. Scalmani, V. Barone, B. Mennucci, G. A. Petersson, H. Nakatsuji, M. Caricato, X. Li, H. P. Hratchian, A. F. Izmaylov, J. Bloino, G. Zheng, J. L. Sonnenberg, M. Hada, M. Ehara, K. Toyota, R. Fukuda, J. Hasegawa, M. Ishida, T. Nakajima, Y. Honda, O. Kitao, H. Nakai, T. Vreven, J. A. Montgomery Jr., J. E. Peralta, F. Ogliaro, M. J. Bearpark, J. Heyd, E. N. Brothers, K. N. Kudin, V. N. Staroverov, R. Kobayashi, J. Normand, K. Raghavachari, A. P. Rendell, J. C. Burant, S. S. Iyengar, J. Tomasi, M. Cossi, N. Rega, N. J. Millam, M. Klene, J. E. Knox, J. B. Cross, V. Bakken, C. Adamo, J. Jaramillo, R. Gomperts, R. E. Stratmann, O. Yazyev, A. J. Austin, R. Cammi, C. Pomelli, J. W. Ochterski, R. L. Martin, K. Morokuma, V. G. Zakrzewski, G. A. Voth, P. Salvador, J. J. Dannenberg, S. Dapprich, A. D. Daniels, Ö. Farkas, J. B. Foresman, J. V. Ortiz, J. Cioslowski and D. J. Fox, Gaussian 09, Gaussian, Inc.: Wallingford, CT, USA, **2009**.